



To What Extent Does Heart Rate Alter the Cerebral Hemodynamic Patterns During Atrial Fibrillation?

Stefania Scarsoglio¹(✉), Luca Ridolfi², Andrea Saglietto³,
and Matteo Anselmino³

¹ Department of Mechanical and Aerospace Engineering, Politecnico di Torino,
Torino, Italy

stefania.scarsoglio@polito.it

² Division of Cardiology, “Città della Salute e della Scienza di Torino” Hospital,
Department of Medical Sciences, Università di Torino, Torino, Italy

³ Department of Environmental, Land and Infrastructure Engineering,
Politecnico di Torino, Torino, Italy

Abstract. Atrial fibrillation (AF), the most common cardiac arrhythmia leading to irregular and faster heartbeat, has been recently and independently associated to the risk of dementia. A constellation of hemodynamic mechanisms has been proposed to explain the possible link between the two pathologies. However, definitive data still miss, and it is unknown how heart rate (HR) influences the cerebral microcirculation. We propose a computational approach, based on a validated hemodynamic modeling, to compare the cerebral circulation during normal sinus rhythm (NSR) and AF at different HRs. AF is able to trigger a higher variability of the cerebral blood flow variables which grows towards the distal circulation. The alteration of the hemodynamic patterns, inducing the rupture of the signal periodicity and the consequent higher occurrence of extremely high/low values, increases with HR. Awaiting necessary clinical evidences, present findings highlight that a strict rate control strategy could be beneficial in terms of cognitive outcomes in patients with permanent AF.

Keywords: Cerebral hemodynamics · Atrial fibrillation · Cardiovascular modelling · Heart rate

1 Introduction

Atrial fibrillation (AF), causing irregular and faster heartbeat, is becoming a public health problem in developing countries [6]. AF has been recently associated with an increased risk of dementia and cognitive decline, even in the absence of clinical cerebrovascular events [3, 4]. Silent cerebral ischemia, microbleeds, and impaired cerebral blood flow have been proposed to explain the link between the two pathologies [2, 5]. Among all possible mechanisms, the alteration of cerebral

perfusion during AF is an aspect which remains poorly investigated so far. In fact, current clinical techniques - such as transcranial doppler ultrasonography - do not provide sufficient resolution to fully describe the inner cerebral circle, in terms of flow and pressure signals. In particular, it is to date unknown whether the irregularity of the RR intervals during AF directly influences cerebral hemodynamics, mostly of the deepest cerebral circulation.

Given the scarcity of clinical data, we recently proposed a computational approach to evaluate the cerebral hemodynamics in AF. It emerged that AF - when compared to the same heart rate (HR) in normal sinus rhythm (NSR) - promotes an altered cerebral hemodynamics and a dramatic signal variation, with the onset of transient hypoperfusions and hypertensive events in the cerebral microcirculation [1, 10, 11].

A signal analysis in terms of cerebral pressure and flow rate time series is here proposed to compare NSR and AF at different HRs, namely from 50 to 130 bpm [7]. In particular, through the percentile and crossing time analyses, we further investigate to what extent the cerebral hemodynamic alterations induced by AF are modulated by means of the heart rate.

2 Methods

2.1 Computational Stochastic Approach

The computational algorithm, as shown in Fig. 1, combines a stochastic extraction of the heart beating, RR [s], with a lumped parameter modeling of the cardiovascular and cerebral circulations. More details, including governing equations, can be found in [7] and therein references.

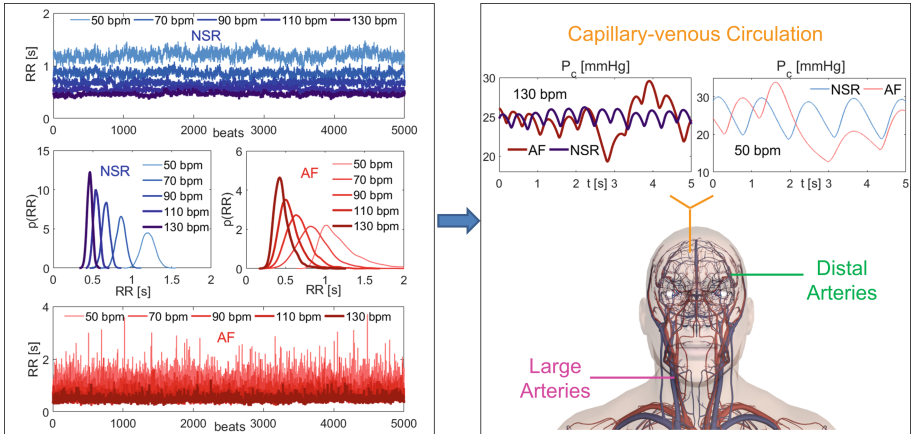


Fig. 1. Scheme of the computational algorithm: (left) RR beats and corresponding probability density functions; (right) Cerebral model with representative capillary pressure signals, P_c .

RR Beating Features in NSR and AF. The artificially extracted RR intervals, based on in vivo beating features and validated over available clinically measured data in NSR and AF [8], span the range of average HR between 50 and 130 bpm. NSR beats are extracted from a Gaussian distribution, which is the typical distribution observed during sinus rhythm. RR extraction is done according to the correlated pink noise temporal structure, the heart rate being a relevant example [8]. Standard deviation values, σ , are determined considering that the coefficients of determination, cv , can be assumed as constant and equal to 0.07 from 50 to 130 bpm. AF distribution can be described by the superposition of two statistically independent times, obtained from a correlated Gaussian and an uncorrelated Exponential distributions. The resulting RR intervals are thus drawn by an exponentially modified Gaussian (EMG) distribution (more details can be found in [8] and therein references). At each HR, the standard deviation, σ , is determined keeping the coefficient of variation, cv , constant and equal to 0.24, while the rate parameter, γ , is taken as a linear function of the mean RR ($\gamma = -9.2RR + 14.6$) [7, 8]. To assure the statistical stationarity of the outcomes, 5000 cardiac cycles are simulated for each configuration. The 5000 beats extracted in NSR and AF conditions and the corresponding RR probability distribution functions are displayed in Fig. 1 (left).

Cardiovascular Model. Once RR intervals are extracted, the cardiovascular model is run to obtain the systemic arterial pressure (P_a). The 0D cardiovascular model, first proposed and validated in AF over more than 30 clinical datasets [8, 9], consists of a network of compliances, resistances and inductances, describing the four contractile cardiac chambers, the systemic and venous circuits. Both atria are imposed as passive to simulate AF conditions, while they can actively contract during NSR. The model includes short-term baroregulation mechanisms [7], accounting for the inotropic effect of both ventricles, as well as the control of the systemic vasculature (peripheral arterial resistances, unstressed volume of the venous system, and venous compliance). The chronotropic effects due to the heart rate regulation, which differently act in NSR and AF, are instead implicitly considered by the RR extraction. The systemic arterial pressure, P_a , is then used as forcing input for the cerebral model.

Cerebral Model. The 0D cerebral model, describing the arterial and venous cerebral circulation, along with the cerebrovascular control mechanisms of autoregulation and CO_2 reactivity [12], has been validated in normal conditions up to the middle cerebral circulation [1], where clinical data are available. A network of compliances and resistances describes the cerebral circulation, which is divided into three main regions: large arteries, distal arterial circulation, and capillary/venous circulation. The left vascular pathway ICA-MCA (i.e., internal carotid artery—middle cerebral artery) is here analyzed as representative of the blood flow and pressure distributions from large arteries to the capillary-venous circulation: left internal carotid artery (systemic arterial pressure, P_a , and left internal carotid flow rate, $Q_{ica,left}$), middle cerebral artery (left middle cerebral

artery pressure, $P_{mca,left}$, and flow rate, $Q_{mca,left}$), middle distal district (left middle distal pressure, $P_{dm,left}$, and flow rate, $Q_{dm,left}$), and capillary-venous circulation (cerebral capillary pressure, P_c , and proximal venous flow rate, Q_{pv}). Figure 1 (right) reports examples of capillary pressures, P_c , in NSR and AF at different HRs.

2.2 Data Analysis

Percentile and crossing time analyses are evaluated for 5000 cycles at different HRs. We here extend the definition of extremely high/low values and the temporal persistence of the hemodynamic signal above/below the physiological threshold during AF [1, 10] to different HRs, so that each rare event during AF is defined as referred to the corresponding NSR at the same HR. NSR outcomes are thus exploited to define the different reference thresholds of each HR [7]. In order to quantify AF-induced variations, the NSR 5th and 95th percentiles of the cerebral hemodynamic variables are taken as reference thresholds for the

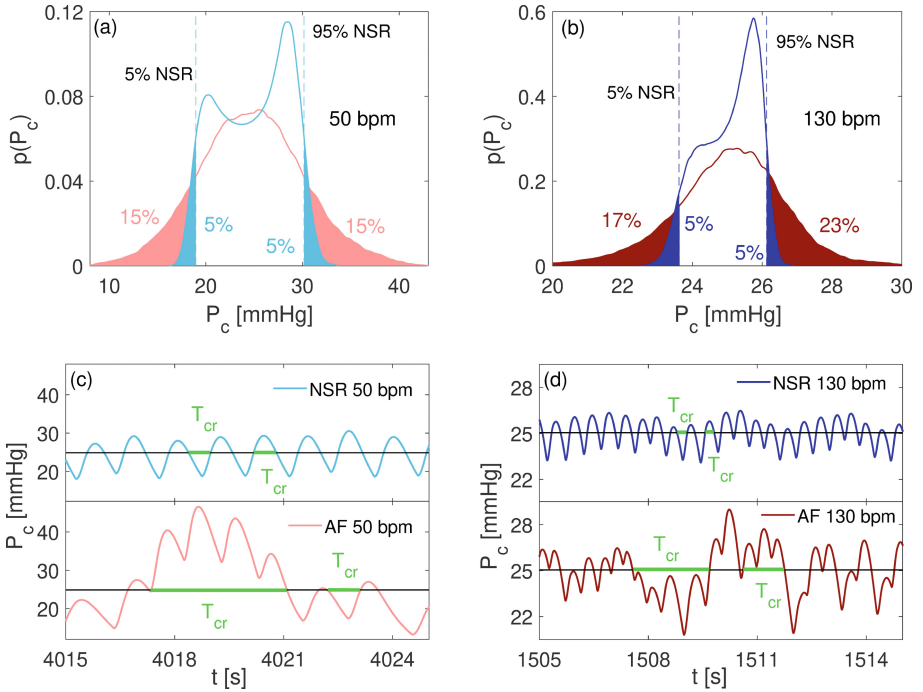


Fig. 2. (a)-(b) Examples of percentile variation for P_c ($p(P_c)$ is the probability density function), at 50 (a) and 130 (b) bpm. NSR thresholds (dashed blue lines) individuate the 5th and 95th percentiles in NSR (blue areas), while they correspond to higher percentiles in AF (red areas). (c)-(d) Examples of T_{cr} evaluation for representative portions of the P_c time series in NSR and AF ((c) 50 bpm, (d) 130 bpm). T_{cr} intervals are indicated in green.

current HR. In AF, we then evaluate to which percentile the NSR reference thresholds correspond, thereby evaluating how AF modifies the probability of assuming extremely high or low values at each fixed HR. Examples of pressure percentile variations between NSR and AF are reported for the capillary region in Fig. 2a and b for $HR = 50$ and 130 bpm, respectively.

Similarly to the percentile analysis, the crossing time evaluation is carried out throughout the whole temporal series at different HRs. At a fixed HR, the crossing time, T_{cr} , is defined as the temporal interval consecutively spent by the hemodynamic variable above or below the threshold individuated at the same HR by the mean value in NSR. In Fig. 2c and d, illustrative examples of T_{cr} are shown for the capillary pressure, P_c , during NSR and AF, at 50 and 130 bpm, respectively. The T_{cr} intervals show, at each HR, how AF influences the duration of excursions from the reference mean value in NSR (individuated at the same HR).

3 Results and Discussion

The alteration of the cerebral hemodynamic signals due to the effect of HR during AF is here investigated, by means of the percentile and crossing time analyses. All the results involve the hemodynamic variables along the selected left ICA-MCA path. We only account for flow rate variations below the 5th percentile (i.e., hypoperfusions) and pressure variations above 95th percentile (hypertensive episodes), since these configurations are the most meaningful from the hemodynamic point of view. For the crossing time analysis, instead, we do not discern whether the time lapse spent is above or below the reference NSR threshold, since both configurations are equally meaningful to evidence the rupture of the signal periodicity and the variation of its temporal pattern.

3.1 Percentile Analysis

The AF percentiles corresponding to the NSR reference thresholds of each HR along the ICA-MCA pathway are reported in Fig. 3. The percentile alteration during AF suggests a worsening - in terms of higher probability of extreme values - in the microcirculation for increasing HR. In fact, at the large artery level ($Q_{ica,left}$, $Q_{mca,left}$, P_a , $P_{mca,left}$) percentile variations are not substantially influenced by the HR - being all confined below the 10th percentile for flow rates (Fig. 3a) and even above the 95th percentile for pressures (Fig. 3b). This last aspect can be explained considering the slight decrease of mean P_a and $P_{mca,left}$ values during AF with respect to NSR, for all the HRs computed [7]. The scenario definitely changes going towards the distal and capillary circulation. Here, not only percentile variations are more marked (up to the 18th and 75th percentiles for flow rates and pressures, respectively), but they also increase with HR. For all the HRs considered, the distal region is the most prone to low perfusion, since the 5th percentile in NSR corresponds to around the 12th–18th percentiles in AF, for $HR = 50$ and 130 bpm, respectively. High pressure levels

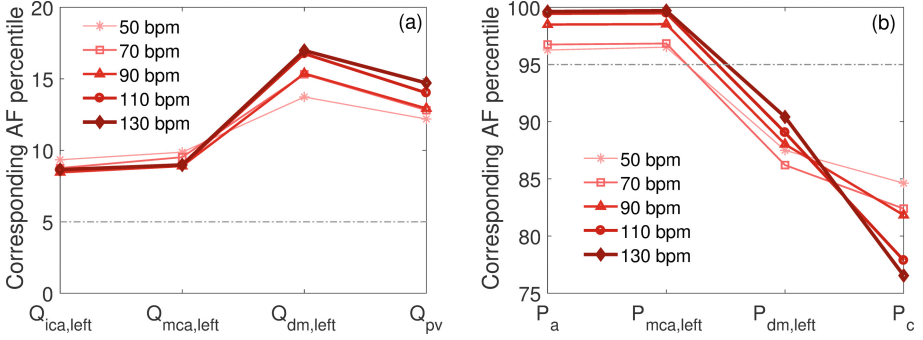


Fig. 3. Percentile analysis corresponding to the NSR threshold of each HR along the ICA-MCA pathway. (a) Flow rate, 5th NSR, (b) Pressure, 95th NSR. Color and thickness (from thin light red to thick dark red) refer to increasing HR (from 50 to 130 bpm), while the abscissa individuates the ICA-MCA regions.

of greater significance are instead more likely to occur in the capillary district, with the 95th NSR percentile corresponding up to the 85th–75th AF percentiles, for HR = 50 and 130 bpm, respectively. Moreover, differently to the large arteries district, mean capillary pressures barely differ between NSR and AF, at all the HRs [7]. Thus, the marked AF percentile variation here observed is all imputable to the greater AF variability, which is not absorbed but even magnified in the microcirculation. What observed so far extends to a wide range of HRs (from 50 to 130 bpm) the higher AF-induced probability of hypoperfusions in the distal region and hypertensive events in the capillary circulation, previously observed only at HR = 70 bpm [1].

3.2 Crossing Time Analysis

The analysis is here presented in terms of the ratio of the mean crossing time in AF, $\mu(T_{cr})_{AF}$, to the mean crossing time in NSR, $\mu(T_{cr})_{NSR}$ (Fig. 4, top panels), and the T_{cr} distributions (Fig. 4, bottom panels). The crossing time analysis shows a behaviour which is qualitatively similar for pressure (left panels) and flow rate (right panels) signals.

For a fixed HR, the ratio $\mu(T_{cr})_{AF}/\mu(T_{cr})_{NSR}$ increases from the proximal to the distal circulation. In particular, in the proximal region the ratio remains unitary, meaning that AF does not modify the signal periodicity and its temporal pattern with respect to NSR. In the distal-capillary compartments, instead, the ratio definitely exceeds one, revealing a higher time lapse spent above/below the reference threshold and thus a pattern alteration. By changing HR, in the proximal region the ratio stays close to one, therefore the HR effect on the signal periodicity and behaviour is negligible. Moving towards the microcirculation, $\mu(T_{cr})_{AF}/\mu(T_{cr})_{NSR}$ ranges from 1.2 (HR = 50 bpm) up to almost 1.8 (HR = 130 bpm). It should be noted that the region mostly involved is the middle distal district ($P_{dm,left}$ and $Q_{dm,left}$), where for HR = 130 bpm crossing times

in AF are on average from 50% to 80% longer than in NSR. This result highlights that, in the deepest cerebral circulation, AF signals at higher HR are more prone to lose their periodicity and alter their temporal structure than those at lower HR. To better explore this last aspect, the probability density functions (PDFs) of T_{cr} where the greatest excursions occur (i. e., middle distal district) are analyzed (see Fig. 4c and d). Even if, at the same HR, the main body of the PDF is similarly positioned in NSR and AF, PDFs during AF display much more pronounced right tails and lose the symmetry shown during NSR. This behaviour becomes more evident when HR is increased from 50 to 130 bpm. The right tails are thus responsible for the increase, as HR grows, of the mean crossing time values in AF with respect to NSR (see the legends of Fig. 4c and d).

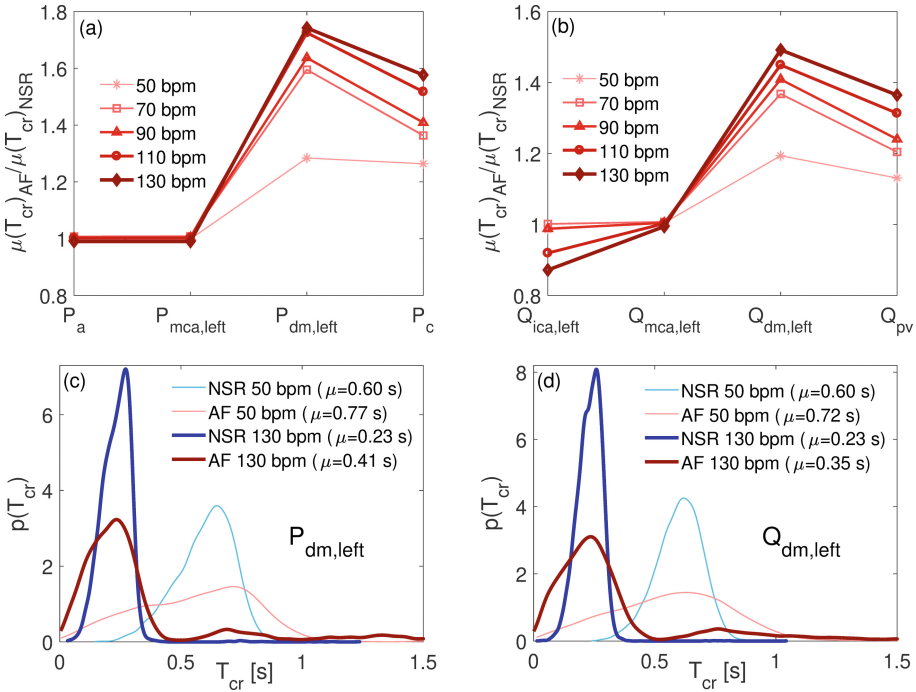


Fig. 4. (a)-(b) Ratio of the mean crossing time in AF, $\mu(T_{cr})_{AF}$, to the mean crossing time in NSR, $\mu(T_{cr})_{NSR}$, at the same HR for (a) pressure and (b) flow rate signals. Color and thickness (from thin light red to thick dark red) refer to increasing HR (from 50 to 130 bpm), while the abscissa individuates the ICA-MCA regions. (c)-(d) Probability density functions (PDFs) of the crossing times, T_{cr} , for (c) $P_{dm,left}$ and (d) $Q_{dm,left}$ during NSR and AF, at 50 and 130 bpm.

4 Conclusions

The present work computationally evaluated how heart rate impacts on the cerebral hemodynamics during AF, through the percentile and crossing time analyses. Critical events - such as the alteration of the cerebral hemodynamic patterns, the loss of the signal periodicity and the related higher occurrence of rare (i.e., extremely high/low) values - emerge in the distal districts and significantly increase in frequency with HR. The trend is basically monotone with HR, thus no optimal HR target to minimize the effects of these transient episodes can be identified. Awaiting further necessary clinical validation and provided that all efforts should be addressed to maintain NSR as long as possible, present findings suggest that a strict rate control strategy could be beneficial in terms of cognitive outcomes in patients with permanent AF.

Acknowledgments. The study was performed thanks to the support of the “Compagnia di San Paolo” within the project “Progetti di Ricerca di Ateneo – 2016: Cerebral hemodynamics during atrial fibrillation (CSTO 160444)” of the University of Turin, Italy.

Conflicts of Interest. The authors declare they have no conflicts of interest.

References

1. Anselmino, M., Scarsoglio, S., Saglietto, A., Gaita, F., Ridolfi, L.: Transient cerebral hypoperfusion and hypertensive events during atrial fibrillation: a plausible mechanism for cognitive impairment. *Sci. Rep.* **6**, 28635 (2016). <https://doi.org/10.1038/srep28635>
2. Da Silva, R.M.F.L., Miranda, C.M., Liu, T., Tse, G., Roevers, L.: Atrial fibrillation and risk of dementia: epidemiology, mechanisms, and effect of anticoagulation. *Front. Neurosci.* **13**, 18 (2019). <https://doi.org/10.3389/fnins.2019.00018>
3. de Bruijn, R.F., Heeringa, J., Wolters, F.J., Franco, O.H., Stricker, B.H., Hofman, A., Koudstaal, P.J., Ikram, M.A.: Association between atrial fibrillation and dementia in the general population. *JAMA Neurol.* **72**(11), 1288–1294 (2015). <https://doi.org/10.1001/jamaneurol.2015.2161>
4. Dietzel, J., Haeusler, K.G., Endres, M.: Does atrial fibrillation cause cognitive decline and dementia? *Europace* **20**(3), 408–419 (2018). <https://doi.org/10.1093/europace/eux031>
5. Jacobs, V., Cutler, M.J., Day, J.D., Bunch, T.J.: Atrial fibrillation and dementia. *Trends Cardiovasc. Med.* **25**(1), 44–51 (2015). <https://doi.org/10.1016/j.tcm.2014.09.002>
6. Morillo, C.A., Banerjee, A., Perel, P., Wood, D., Jouven, X.: Atrial fibrillation: the current epidemic. *J. Geriatr. Cardiol.* **14**(3), 195–203 (2017). <https://doi.org/10.11909/j.issn.1671-5411.2017.03.011>
7. Saglietto, A., Scarsoglio, S., Ridolfi, L., Gaita, F., Anselmino, M.: Higher ventricular rate during atrial fibrillation relates to increased cerebral hypoperfusions and hypertensive events. *Sci. Rep.* **9**, 3779 (2019). <https://doi.org/10.1038/s41598-019-40445-5>

8. Scarsoglio, S., Guala, A., Camporeale, C., Ridolfi, L.: Impact of atrial fibrillation on the cardiovascular system through a lumped-parameter approach. *Med. Biol. Eng. Comput.* **52**(11), 905–920 (2014). <https://doi.org/10.1007/s11517-014-1192-4>
9. Scarsoglio, S., Camporeale, C., Guala, A., Ridolfi, L.: Fluid dynamics of heart valves during atrial fibrillation: a lumped parameter-based approach. *Comput. Methods Biomech. Biomed. Eng.* **19**(10), 1060–1068 (2016). <https://doi.org/10.1080/10255842.2015.1094800>
10. Scarsoglio, S., Saglietto, A., Anselmino, M., Gaita, F., Ridolfi, L.: Alteration of cerebrovascular haemodynamic patterns due to atrial fibrillation: an in silico investigation. *J. Roy. Soc. Interface* **14**(129), 20170180 (2017). <https://doi.org/10.1098/rsif.2017.0180>
11. Scarsoglio, S., Cazzato, F., Ridolfi, L.: From time-series to complex networks: application to the cerebrovascular flow patterns in atrial fibrillation. *Chaos* **27**(9), 093107 (2017). <https://doi.org/10.1063/1.5003791>
12. Ursino, M., Giannessi, M.: A model of cerebrovascular reactivity including the circle of willis and cortical anastomoses. *Ann. Biomed. Eng.* **38**(3), 955–974 (2010). <https://doi.org/10.1007/s10439-010-9923-7>